WILEY

Research Article

Repurposing the Antibacterial Activity of the Drug Teniposide Against Gram-Positive Bacteria

Federica Dell'Annunziata [1,2] Veronica Folliero [1] Roberta Della Marca [2] Francesca Palma [2] Giuseppina Sanna [3] Anna De Filippis [2] Pasquale Pagliano [1] Aldo Manzin [3] Gianluigi Franci [1,4] and Massimiliano Galdiero [2,5]

[1]*Department of Medicine, Surgery and Dentistry Scuola Medica Salernitana, University of Salerno, 84081 Salerno, Italy*
[2]*Department of Experimental Medicine, University of Campania "Luigi Vanvitelli", 80138 Naples, Italy*
[3]*Department of Biomedical Sciences, Microbiology and Virology Unit, University of Cagliari, 09042 Cittadella Universitaria, Monserrato, Italy*
[4]*Clinical Pathology and Microbiology Unit, San Giovanni di Dio e Ruggi D'Aragona University Hospital, 84126 Salerno, Italy*
[5]*Complex Operative Unity of Virology and Microbiology, University Hospital of Campania "Luigi Vanvitelli", 80138 Naples, Italy*

Correspondence should be addressed to Gianluigi Franci; gfranci@unisa.it
and Massimiliano Galdiero; massimiliano.galdiero@unicampania.it

Drug repurposing is sparking considerable interest due to reduced costs and development times. The current study details the screening of teniposide, an antitumor drug, for its antibacterial activity against both Gram-positive and Gram-negative strains, with a focus on *Staphylococcus epidermidis* (*S. epidermidis*), the primary causative agent of nosocomial and transplant-related infections. The cytotoxicity was evaluated through 3-(4,5-dimethylthiazol-2-yl)-2,5-diphenyl tetrazolium bromide (MTT) and hemolysis assays on immortalized human keratinocyte (HaCaT) cells and human erythrocytes. After 20 h of treatment, the recorded concentrations causing 50% cytotoxicity (CC_{50}) and hemolysis (HC_{50}) were 33.63 and 121.55 µg/mL, respectively. The antibacterial screening employed disk diffusion, the broth microdilution method, LIVE/DEAD staining, and a time-killing test. The drug induced a growth inhibitory area in the 22–25 mm range for all Gram-positive strains. The minimum concentration that inhibited 90% of bacteria (MIC_{90}) was 6.25 µg/mL against *Staphylococcus aureus* and *S. epidermidis* and 12.5 µg/mL versus *Enterococcus faecalis*, exhibiting bactericidal action. Treatment resulted in *S. epidermidis* cell morphology deformities and damage to the cell membrane, observed by scanning electron microscopy (SEM). Mechanism analysis revealed alterations in the selective permeability of the cell membrane, observed under the fluorescence microscope by the absorption of propidium iodide (PI). The synergistic effect of teniposide in combination with fosfomycin and gentamicin was documented by disk diffusion and checkboard assay, recording a fractional inhibitory concentration index (FICI) of 0.28 and 0.37, respectively. The drug's action on *S. epidermidis* biofilm biomass was investigated using crystal violet (CV) and MTT. Teniposide affected biofilm viability in a dose-dependent manner, inducing, at a concentration of 3.12 µg/mL, a matrix inhibition of about 42% and 61%, with a sessile metabolic activity of 54% and 24% recorded after 2 and 24 h, respectively. Overall, this study suggests the potential repurposing of the anticancer drug teniposide as a therapeutic agent to counteract *S. epidermidis* infections.

Keywords: antibacterial activity; biofilm inhibition; drug repurposing; multidrug resistance; *S. epidermidis*; teniposide

Summary

- *S. epidermidis* is a worrying pathogen in healthcare-associated infections, especially in medical device–related contamination.

- *S. epidermidis* strains represent a serious threat due to multidrug resistance, and the production of biofilm further complicates treatment, reducing the effectiveness of antibiotics.

- Challenges related to the development of new drugs are necessary for innovative therapeutic options that counteract MDR *S. epidermidis* infections.

- The study investigates the antimicrobial potential of teniposide, a Food and Drug Administration (FDA)-approved anticancer drug. The research explores the possibility of drug-repurposing teniposide as a potent antimicrobial agent against susceptible and MDR *S. epidermidis*.
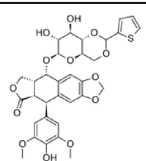
1. Introduction

Staphylococcus epidermidis (*S. epidermidis*) is a coagulase-negative staphylococcus (CoNS) bacterium, a component of human and animal skin microbiota [1]. It is recognized as a causative agent of healthcare-associated infections, mainly medical device–related contaminations [2]. *S. epidermidis* infections typically manifest after extended periods of hospitalization and after surgical implantation procedures [3]. As of 2020, the World Health Organization (WHO) estimated that approximately seven out of 100 patients in developed countries and 10 out of 100 patients in underdeveloped countries encounter multidrug-resistant (MDR) *S. epidermidis* during hospitalization [4]. Among these cases, about 50%–70% of strains are associated with medical devices, predominantly affecting immunocompromised patients [4]. The pathogenesis of *S. epidermidis* is influenced by several factors: (i) biofilm formation on both biotic and abiotic surfaces [5], (ii) secretion of enzymes and extracellular toxins [6], (iii) invasive capacity and intracellular persistence [7], and (iv) modulation of the host immune system [8]. Additionally, the disproportionate use of antibiotics associated with the limited availability of new molecules has contributed to a rising trend of MDR strains, posing challenges in managing and treating nosocomial infections [9]. To date, *S. epidermidis* has gained resistance to several classes of antibiotics including beta-lactams, aminoglycosides, macrolides, and, to a lesser extent, tetracyclines, amphenicols, and lincosamides [10]. A study conducted by Majeed et al. reported the sensitivity profiles to different classes of antibiotics in 38 MDR *S. epidermidis* isolates, noting resistances for fosfomycin (89.47%), amoxicillin (78.94%), cefoxitin (73.68%), oxacillin (55.25%), cephradine (21.05%), and vancomycin (15.78%) [11]. To worsen the scenario, antimicrobial resistance is enhanced by the strong biofilm production of *S. epidermidis*, which reduces antibiotic penetration and favors the exchange of gene determinants through mechanisms of horizontal gene transfer [12, 13]. Our previous investigations revealed a strong association between the multidrug resistance profile and biofilm production. Specifically, out of a sample of 76 medical devices, 33.0% of the isolated strains belonged to the CoNS category, of which *S. epidermidis* represented 54.8%. Among these strains, 64.7% demonstrated an multidrug resistance profile, while 35.3% were non multidrug resistance. Among the MDR strains, 90.1% showed biofilm production capabilities. In detail, 36.4%, 45.5%, and 9.1% were identified as strong, medium, and weak biofilm producers, respectively. Biofilm-producing MDR strains have shown resistance rates greater than 50% against ampicillin, trimethoprim–sulfamethoxazole, tetracycline, oxacillin, moxifloxacin, gentamicin, erythromycin, ciprofloxacin, and fusidic acid. Among non-MDR strains, a significant majority (83.3%) were identified as nonbiofilm producers. The latter exhibited high sensitivity rates, above 60%, for antibiotics such as fusidic acid, ciprofloxacin, clindamycin, daptomycin, erythromycin, fosfomycin, gentamicin, linezolid, moxifloxacin, oxacillin, teicoplanin, tetracycline, tigecycline, trimethoprim–sulfamethoxazole, and vancomycin [14]. In this constant challenge, the need for new therapeutic options worldwide has become evident [15]. However, it is well known that the economic and managerial efforts required to discover new drugs, coupled with long research and development times, are unlikely to deliver innovative therapies promptly [16]. The current winning strategy implemented by research centers and exploited by pharmaceutical companies is drug repurposing [17–19].

Pharmacological repurposing involves identifying novel potential applications for drugs that have already received regulatory approval [20]. It relies on two fundamental principles: (i) certain diseases share common molecular pathways or underlying predisposing factors [21]; (ii) numerous drugs possess hidden or latent functions that may manifest in specific contexts [22]. Our previous studies successfully reported the drug repurposing of anthelmintic drugs (selamectin, ivermectin, doramectin, and niclosamide) against clinical isolates of MDR *Corynebacterium striatum* and the secondary metabolite rhein (4,5′-dihydroxy-anthraquinone-2-carboxylic acid) against *Streptococcus mutans* and *Staphylococcus aureus* [23–26]. Contextually, the present manuscript investigated the antimicrobial potential of teniposide, a derivative of podophyllotoxin, as etoposide (VP-16), etoposide phosphate (etopophos), and azatoxin [27]. Teniposide was approved as an anticancer drug by the Food and Drug Administration (FDA) in 1992 and is used in the treatment of acute lymphoblastic leukemia in both children and adults [28]. In adulthood, it is also employed in the treatment of non-Hodgkin's lymphoma. Despite the numerous studies on the teniposide effects and mechanism of action in eukaryotic cells, its antimicrobial properties are not widely investigated [29, 30]. Therefore, antimicrobial screening against several Gram-positive and Gram-negative bacteria was conducted, with a focus on susceptible and MDR strains of *S. epidermidis*. Our encouraging results establish a solid foundation for understanding the role of the chemotherapy drug teniposide as a potent antimicrobial agent.

TABLE 1: Chemical structure and molecular properties of teniposide.

	Teniposide
Chemical structure	
Molecular formula	$C_{32}H_{32}O_{13}S$
Molecular weight	656.65 g/mol
Appearance	White to off-white
Density	$1.6 \pm 0.1 \, \text{g/cm}^3$
Melting point	242°C–246°C
Boiling point	$864.3 \pm 65.0°C$
Solubility in DMSO	$1.59 \, \text{g/cm}^3$

TABLE 2: Multisensitive bacteria used in the study.

Gram-positive	Gram-negative
Staphylococcus aureus ATCC 6538	*Escherichia coli* ATCC 11229
Staphylococcus epidermidis ATCC 12228	*Klebsiella pneumoniae* ATCC 10031
Staphylococcus epidermidis ATCC 35984	
Enterococcus faecalis ATCC 29212	*Salmonella enterica* ser. Typhimurium ATCC 14028

2. Material and Methods

2.1. Samples and Concentrations Tested.
Teniposide is a semisynthetic molecule derived from podophyllotoxin with proven antineoplastic activity (Table 1). The teniposide used in this study was purchased from Sigma-Aldrich (St. Louis, MO, United States). The colourless soluble powder was dissolved in dimethyl sulfoxide (DMSO, Sigma-Aldrich, St. Louis, MO, United States) to a final concentration of 5 mg/mL and stored at −20°C until use.

2.2. Cell Cultures and Cytotoxicity Assays.
Immortalized human keratinocyte (HaCaT) cells were utilized to evaluate the cytotoxicity of teniposide through the 3-(4,5-dimethyl-thiazol-2-yl)-2,5-diphenyl tetrazolium bromide (MTT, Sigma-Aldrich, St. Louis, MO, United States) assay. Cells were cultured in Dulbecco's Modified Eagle Medium (DMEM, Microgem, Pozzuoli, IT), supplemented with 1% penicillin–streptomycin and 10% bovine serum, at 37% C with 5% CO_2 in a humid environment. Cells (2×10^4/well) were seeded into 96-well plates and incubated for 24 h. Teniposide was tested in a concentration range of 100–1.56 μg/mL. Cells treated with solvent at the concentration used to dissolve the compound (2% DMSO) and cells treated with 100% DMSO represented control negative (CTRL−) and positive (CTRL+), respectively. After the exposure time, the culture medium was removed, and 100 μL of MTT solution (0.3 mg/mL) was added to each well for 3 h at 37°C. The formazan crystals were subsequently solubilized with 100 μL of 100% DMSO, and the cytotoxic effect was evaluated by measuring the absorbance at 570 nm. To better understand the cytotoxic effect on human cells, the hemolytic activity was determined using fresh human erythrocytes from healthy anonymous donors. Briefly, 25 mL of blood was centrifuged, and the erythrocytes were washed three times with NaCl solution (150 mM). Then, blood was diluted 1:50 in phosphate-buffered saline 1× (PBS, Sigma-Aldrich, St. Louis, MO, United States), pH 7.4, and 180 μL of red blood cell solution was added to the well of a 96-well conical bottom. Teniposide was exposed at the same concentrations mentioned above; the solvent (2% DMSO) and 0.1% Triton X

solution represented CTRL− and CTRL+. The samples were incubated under orbital shaking at 37°C for 2 h and then centrifuged at 500 rpm for 5 min. Hemoglobin release was monitored by measuring the supernatant optical density at 540 nm.

2.3. Bacterial Strains and Growth Conditions.
All multisensitive bacteria selected in the study (Table 2) were purchased from the American Type Culture Collection (ATCC, Manassas, VA, United States). Ten clinical isolates of *S. epidermidis* (Table 3) were collected at the "Luigi Vanvitelli" University Hospital of Campania (Naples, IT). Clinical strains were plated on trypticase soy agar plates with 5% horse blood (Oxoid, Hampshire, MA, United States). The bacterial species were identified by MALDI-TOF mass spectrometry (Bruker Daltonics, Bremen, DE), and the antibiotic resistance profile was evaluated using the Phoenix BD system (Becton Dickinson, Franklin Lakes, NJ, United States). To evaluate the teniposide antibacterial effect, the bacteria were seeded on Muller–Hinton (MH) agar (Sigma-Aldrich, St. Louis, MO, United States) plates and the bacterial suspension useful for antibacterial assays was prepared in MH broth (Sigma-Aldrich, St. Louis, MO, United States). Furthermore, the compound's ability to impact the biofilm matrix was evaluated by plating bacteria onto Luria–Bertani (LB) agar (Sigma-Aldrich, St. Louis, MO, United States) plates and preparing inoculum in LB broth (Sigma-Aldrich, St. Louis, MO, United States).

2.4. Kirby–Bauer Disk Diffusion Test.
Antibacterial susceptibility was evaluated by the Kirby–Bauer disk diffusion test, following the guidelines of the National Committee on Clinical Laboratory Standards (NCCLS). Briefly, a fresh colony of each strain grown on the MH agar plate was inoculated in saline to a turbidity of 0.5 McFarland. The bacterial suspensions were seeded uniformly with a sterile swab on a MH agar plate. A blank disk (Oxoid, Hampshire, MA, United States) with 50 μg of teniposide (10 μL) was placed on a MH agar plate and incubated at 37°C. Piperacillin (30 μg) and linezolid (10 μg) (Oxoid, Hampshire, MA, United States) were used as CTRL+ for Gram-negative and Gram-positive, respectively, while a 100% DMSO-soaked disk (10 μL) was used as a solvent control. After 24 h of incubation, the diameters of the inhibition areas were measured.

2.5. Determination of the Minimum Inhibitory Concentration.
The antibacterial activity of teniposide was evaluated against

TABLE 3: Susceptibility profile of *S. epidermidis* collected clinical strains.

	FUS	CIP	CLI	DAP	ERI	FOS	GEN	LIN	MOX	OXA	TEI	TET	TIG	TRI	VAN
S. epidermidis-1	S	R	R	S	R	S	R	S	R	R	S	S	S	R	S
S. epidermidis-2	R	S	S	S	R	S	R	S	S	R	S	R	S	S	S
S. epidermidis-3	R	S	R	S	S	S	R	S	S	R	S	S	S	S	S
S. epidermidis-4	R	R	S	S	S	S	R	S	R	R	S	S	S	R	S
S. epidermidis-5	S	R	R	S	R	S	S	S	R	R	S	S	S	S	S
S. epidermidis-6	S	R	S	S	S	S	S	S	R	S	S	I	S	R	S
S. epidermidis-7	S	R	S	S	S	S	S	S	R	R	S	S	S	R	S
S. epidermidis-8	S	R	S	S	R	R	R	S	R	R	S	R	R	R	S
S. epidermidis-9	S	R	R	S	R	S	R	S	R	R	S	R	S	R	S
S. epidermidis-10	R	R	I	S	R	R	R	S	R	R	S	S	S	R	S

Note: Clinical breakpoints are reported for each antibiotic in accordance with the European Committee on Antimicrobial Susceptibility Testing (EUCAST) guidelines.

Abbreviations: CIP: ciprofloxacin (<4 U/mL); CLI: clindamycin (≤0.25 U/mL); DAP: daptomycin (≤0.5 U/mL); ERI: erythromycin (≤0.25 U/mL); FOS: fosfomycin c/G6P (≤ U/mL); FUS: fusidic acid (<8 U/mL); GEN: gentamicin (<4 U/mL); LIN: linezolid (<2 U/mL); MOX: moxifloxacin (<1 U/mL); OXA: oxacillin (<2 U/mL); "R": resistance; "S": susceptible; TEI: teicoplanin (≤2 U/mL); TET: tetracycline (<1 U/mL); TIG: tigecycline (≤0.25 U/mL); TRI: trimethoprim–sulfamethoxazole (<0.05 U/mL); VAN: vancomycin (<1 U/mL).

all selected bacteria. Fresh colonies of each strain grown on MH agar were inoculated in MH broth and incubated overnight (ON) at 37°C. The bacterial suspension was resuspended in a fresh medium and further incubated at 37°C until the exponential growth phase (1×10^8 CFU/mL). Then, serial dilutions were performed to obtain the bacterial concentration required for the test (1×10^6 CFU/mL). The plate microdilution method was conducted in a 96-well plate by adding 10 μL of the compound diluted in 1× PBS, in the concentration range 100–1.56 μg/mL, 40 μL of MH broth, and 50 μL of bacterial suspension (1×10^6 CFU/mL). Ciprofloxacin (0.01 μg/mL) for *Pseudomonas aeruginosa*, ampicillin (20 μg/mL) for *Escherichia coli* and *Klebsiella pneumoniae*, and vancomycin (10.4 μg/mL) for Gram-positive strains were used as CTRL+, while bacteria treated with 1% DMSO, which represented the highest concentration of solvent used, represented the CTRL−. The antimicrobial activity of the compounds was evaluated after 24 h of incubation at 37°C under vigorous orbital shaking. Bacterial growth was monitored by measuring the absorbance at 600 nm, and the percentage of inhibition was calculated according to the following formula:

$$\%\text{Growth inhibition} = 100 - \left[\frac{(100 \times \text{OD600 nm of the test sample})}{\text{OD600 nm of CTRL} -} \right]$$

2.6. Time-Kill Kinetics Assay.

To better understand the teniposide kinetics against *S. epidermidis*, bacterial growth was monitored over time. Doses of 1/2× MIC (3.12 μg/mL), 1× MIC (6.25 μg/mL), and 2× MIC (12.5 μg/mL) were added to the MH broth in a final volume of 2 mL. Untreated bacteria and vancomycin-treated bacteria were used as CTRL− and CTRL+, respectively. A bacterial suspension of 1×10^6 CFU/mL was added to each tube and incubated at 37°C with orbital shaking (180 rpm). A volume of 100 μL at time intervals of 0, 2, 4, 6, and 20 h was serially diluted in 1× PBS, and 20 μL of each dilution was plotted on MH agar and incubated at

TABLE 4: FICI values indicating synergism, additivity, and antagonism.

Combinatorial effect	FICI value
Synergism	≤0.5
Addivism	$0.5 < F \leq 1.0$
Indifference	$1 < F \leq 4$
Antagonism	>4.0

37°C. The following day, colonies were counted to determine the CFU/mL.

2.7. Scanning Electron Microscopy (SEM).

The morphological changes against *S. epidermidis* were observed by SEM. Teniposide bacterial treatment at 1/2× MIC (3.12 μg/mL) and 1× MIC (6.25 μg/mL) was performed as described in Section 2.5. Unexposed and vancomycin-treated bacterial cells represented CTRL− and CTRL+, respectively. After exposure, the bacterial pellets were washed twice in 1× PBS and fixed in 2.5% glutaraldehyde. Then, the bacteria were dehydrated with ethanol solutions (25%, 50%, 70%, 95%, and 100% v/v). Images were acquired using the ZEISS Supra 40 at an accelerating voltage of 5 kV with the Everhart–Thornley Detector (ETD) and through lens detector (TLD) set at 10,000, 20,000, and 50,000× magnifications (EHT = 5.00 kV, WD = 22 mm, the detector in the objective) (Berlin, DE).

2.8. LIVE/DEAD Staining.

Following the results obtained from the time-kill kinetics assay, bacteria treated with different teniposide concentrations for 6 h were examined for cell viability using a BacLight LIVE/DEAD staining kit (Invitrogen, Carlsbad, United States). According to the manufacturer's instructions, equal volumes of SYTO® 9 and propidium iodide (PI) were mixed and added to each 96-well plate well. The samples were incubated for 15 min in the dark at room temperature and observed under a fluorescence microscope
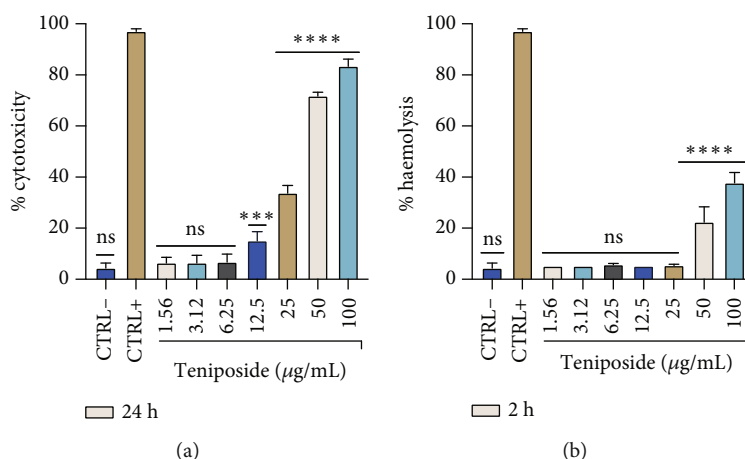
FIGURE 1: (a) HaCaT cytotoxicity after 24 h of exposure to teniposide. (b) Hemolysis after exposure of human red blood cells to compound. The CTRL− was represented by the solvent-treated cells used to dissolve the drug (2% DMSO); CTRL+ was represented by DMSO used at toxic concentrations (100%) for the MTT test and 0.1% TritonX-100 for the hemolysis test. Dunnett's multiple comparison test: ****p value < 0.0001; ***p value < 0.0007; ns p value > 0.05. Ordinary one-way ANOVA: p value < 0.0001; R − squared = 0.9871.

[31]. The images were taken using the Nikon ECLIPSE Ti2-U (Nikon Europe B.V., Amsterdam, Netherlands) inverted fluorescence microscope with beam settings for FITC and TRITC and merged.

2.9. Double-Disk Synergy and Checkerboard Assay. To evaluate the teniposide combinatorial effect with common antibiotics, a double-disk synergy screening was performed using rifampicin (5 μg), fosfomycin (200 μg), gentamicin (10 μg), clarithromycin (15 μg), linezolid (10 μg), chloramphenicol (30 μg), cefoxitin (30 μg), ampicillin (2 μg), ciprofloxacin (5 μg), tigecycline (15 μg), norfloxacin (10 μg), and meropenem (10 μg) (Thermo Fisher Scientific, Massachusetts, United States), as representative antibiotics of each class. The bacterium at a density of 0.5 McFarland was seeded on a MH agar plate using a sterile swab. Then, each antibiotic was placed at 2 cm with the disk soaked in teniposide (50 μg) and incubated for 24 h at 37°C. Potential synergism (crossing of halos), antagonism (repelling of halos), and indifference/additivism (adjacency of halos) were evaluated, and the best combinations were confirmed through the checkerboard assay [32]. For this test, the microdilution plate method determined the exact MIC value for the antibiotics clarithromycin, ciprofloxacin, fosfomycin, and gentamicin. Then, the antibiotic combinations (clarithromycin 2–0.002 μg/mL, ciprofloxacin 0.2–0.0001 μg/mL, fosfomycin 64–0.12 μg/mL, and gentamicin 8–0.01 μg/mL) and teniposide (12.5–0.19 μg/mL) were added to each well of the 96-well plate. The bacterial inoculum at a density of 1×10^6 CFU/mL was added to the compounds tested alone and in combination. The plates were incubated at 37°C under orbital shaking (180 rpm) for 20 h, and then bacterial growth was measured spectrophotometrically (600 nm). The combinatorial effect was analyzed by calculating the fractional inhibitory concentration index (FICI) according to the following formula: FICI = (MIC A in combination)/(MIC A alone) + (MIC B in combination)/(MIC B alone).

The antibiotic/teniposide combinatorial effect was evaluated considering the FICI values reported in Table 4.

2.10. Biofilm Inhibition. The biofilm inhibitory effect of teniposide was investigated in the initial formation stages (2 h) and the maturation (24 h) phases against *S. epidermidis* ATCC and two clinical isolates (*S. epidermidis*$_{S1-S2}$). Then, the bacterial inoculum of each strain was diluted to OD 600 nm = 0.2 (2×10^8 CFU/mL) in LB broth supplemented with 1% glucose and exposed to compound (50–0.39 μg/mL) in a final volume of 200 μL. The unexposed bacterium represented CTRL−. After treatment, the matrix was washed twice in 1× PBS to remove planktonic cells and stained with 0.05% crystal violet (CV) for 40 min. The excess CV was discarded, and the dye trapped in the matrix was solubilized with 100% ethanol for 10 min. The absorbance recorded at 570 nm defined the percentage of inhibited matrix according to the following formula:

$$\%\text{Biofilm inhibition} = 1 - \left(\frac{\text{DO570 nm of test sample}}{\text{OD570 nm of CTR} -} \right) \times 100$$

The experiment was conducted under the same conditions to evaluate the percentage of viable cells present in the inhibited matrix using the MTT assay. After the teniposide exposure time (2 and 24 h), the matrix was washed twice in 1× PBS and treated with a 0.5 mg/mL MTT solution for 3 h at 37°C. Then, the formed formazan crystals were solubilized with 100% DMSO for 10 min. The absorbance read at 570 nm defined the percentage of metabolically active cells according to the following formula:

$$\%\text{Metabolic activity} = \left[\frac{(100 \times \text{OD 570 nm of test sample})}{\text{OD 570 nm of CTR} -} \right]$$
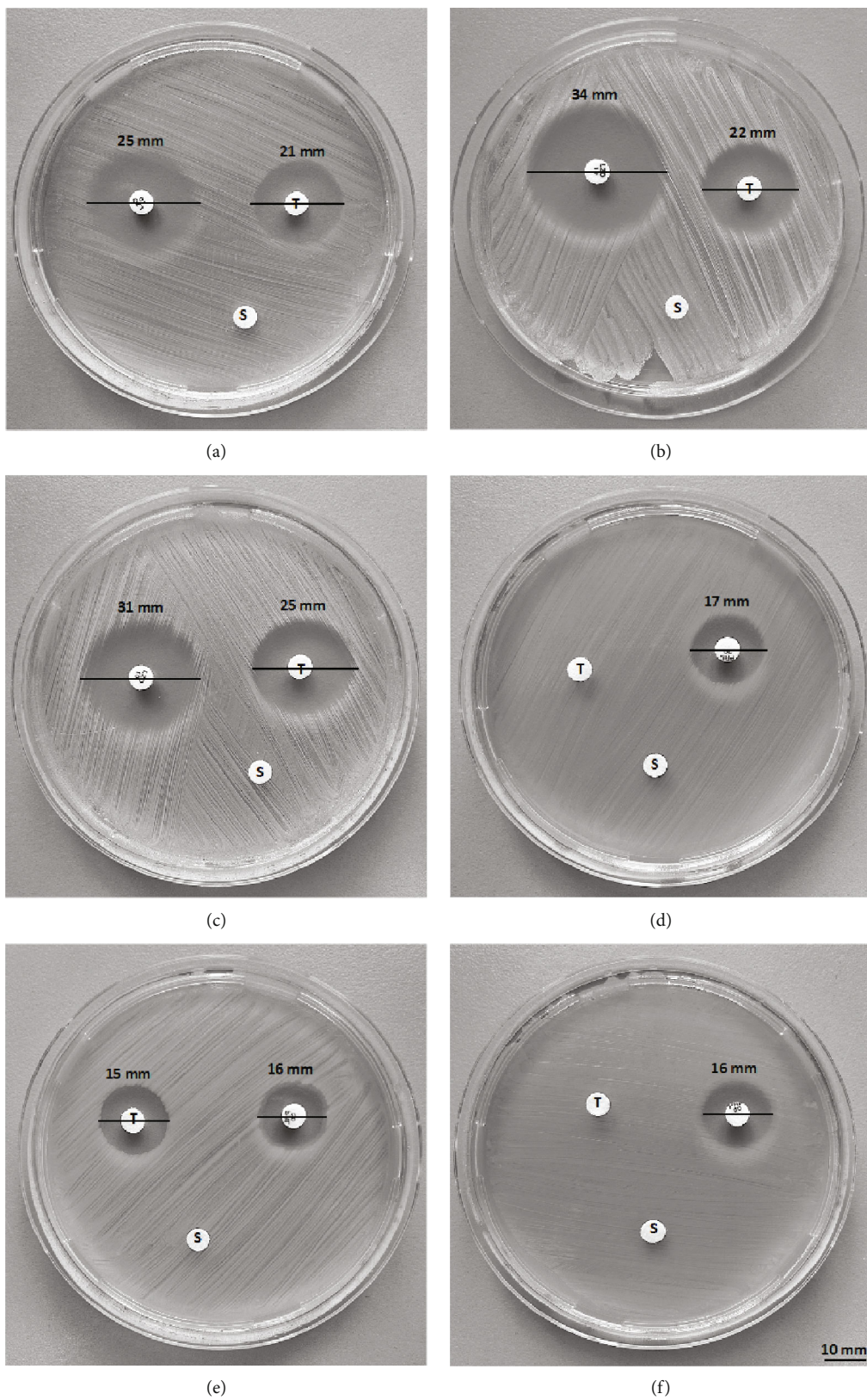
(a)

(b)

(c)

(d)

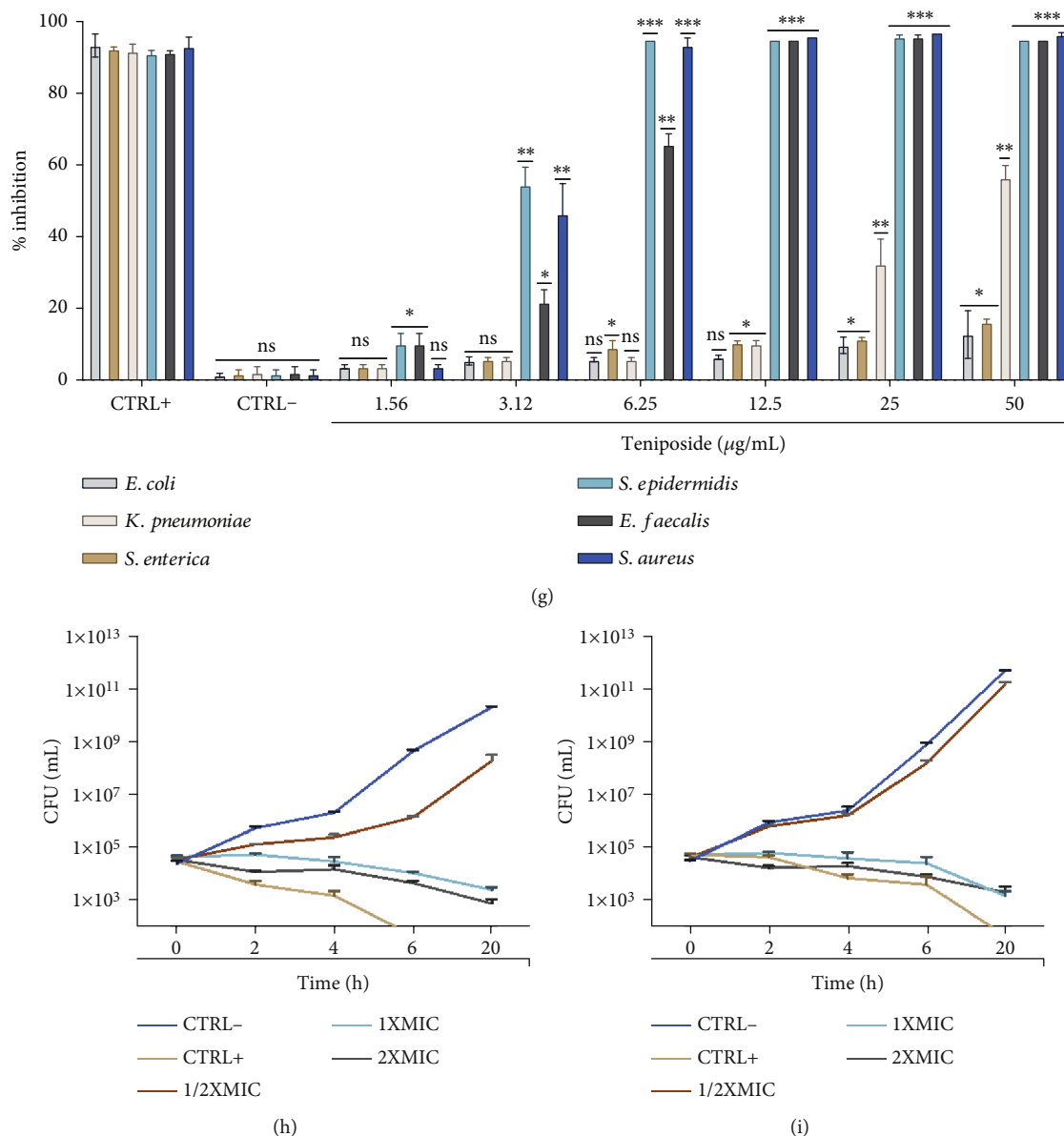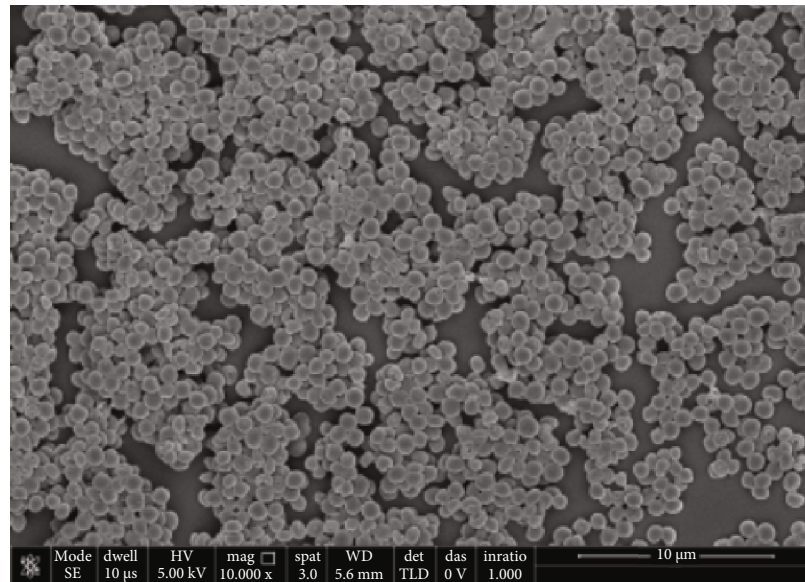

(e)

(f)

FIGURE 2: Continued.

FIGURE 2: Antibacterial screening of teniposide (50 μg) against (a) *E. faecalis*, (b) *S. aureus*, (c) *S. epidermidis*, (d) *E. coli*, (e) *K. pneumoniae*, and (f) *S. enterica* ser. Typhimurium. Linezolid (10 μg) and piperacillin (30 μg) represented the CTRL+ against Gram-positive and Gram-negative bacteria, respectively. The solvent control was represented by a 100% DMSO-soaked disk (10 μL). (g) Antibacterial activity of teniposide against selected bacteria by the broth microdilution method. Time-kill kinetics of teniposide against (h) *S. epidermidis* ATCC 12228 and (i) clinical isolate S_1. The CTRL− was represented by the solvent-treated cells used to dissolve the drug (2% DMSO); ciprofloxacin (0.01 μg/mL), ampicillin (20 μg/mL), and vancomycin (10.4 μg/mL) represented CTRL+ for Gram-negative and Gram-positive bacteria. Dunnett's multiple comparison test: ***p value < 0.0003; **p value < 0.0041; *p value < 0.0364; ns p value > 0.05. Ordinary one-way ANOVA: p value < 0.0005; R − squared = 0.9971.

2.11. Statistical Analysis. Each experiment conducted included three technical replicas and two biological duplicates. All the data collected were expressed as the mean ± standard deviation (SD). Minimal growth inhibition concentrations of 50% and 90% (MIC_{50} and MIC_{90}) and cytotoxic and hemolysis concentrations of 50% (CC_{50} and HC_{50}) were calculated using the GraphPad Software Prism 9.0 (San Diego, CA, United States). The significance of the difference between 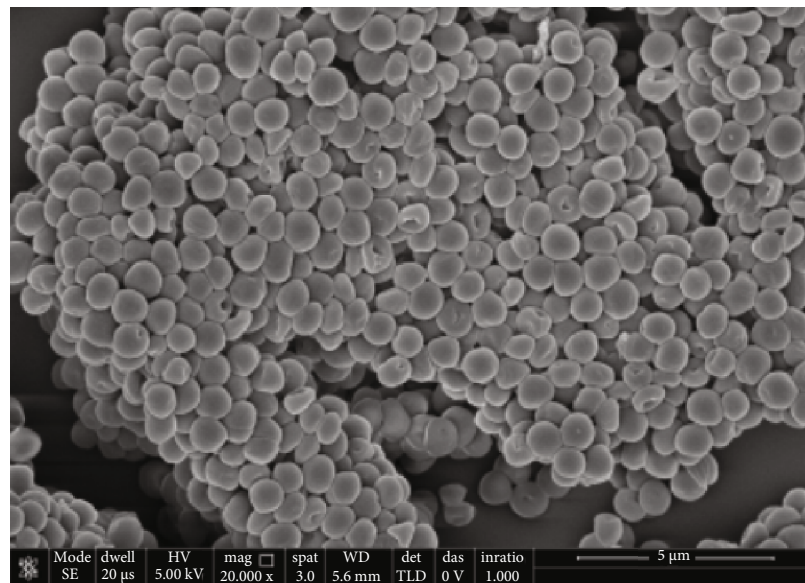treated- and CTRL−-samples was obtained with Dunnett's test and ANOVA analysis. A p value < 0.05 was considered significant.

3. Results

3.1. Cytotoxicity on Human Cells. The teniposide effect on the HaCaT cell line and human red blood cells was evaluated by MTT and hemolysis tests, respectively. After 24 h of exposure, cytotoxicity was established at the highest
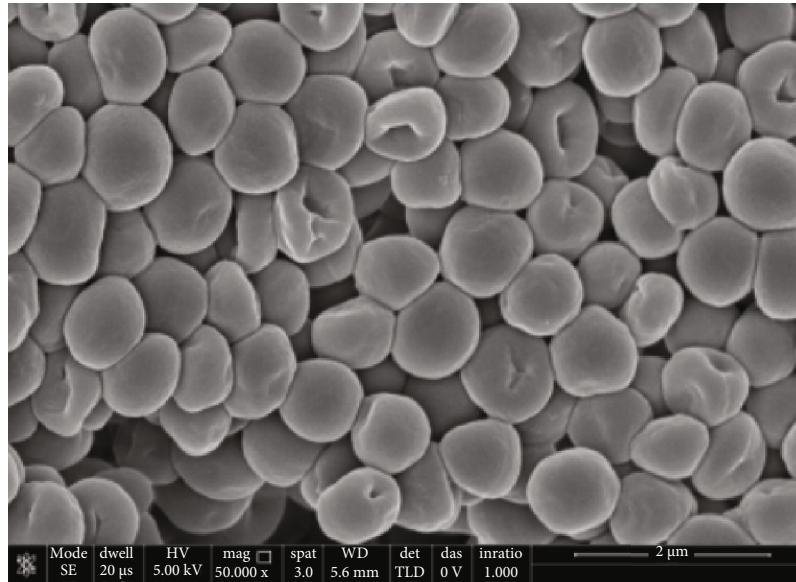
| Mode | dwell | HV | mag ▫ | spat | WD | det | das | inratio | 10 μm |
| SE | 10 μs | 5.00 kV | 10.000 x | 3.0 | 5.6 mm | TLD | 0 V | 1.000 | |

(a)

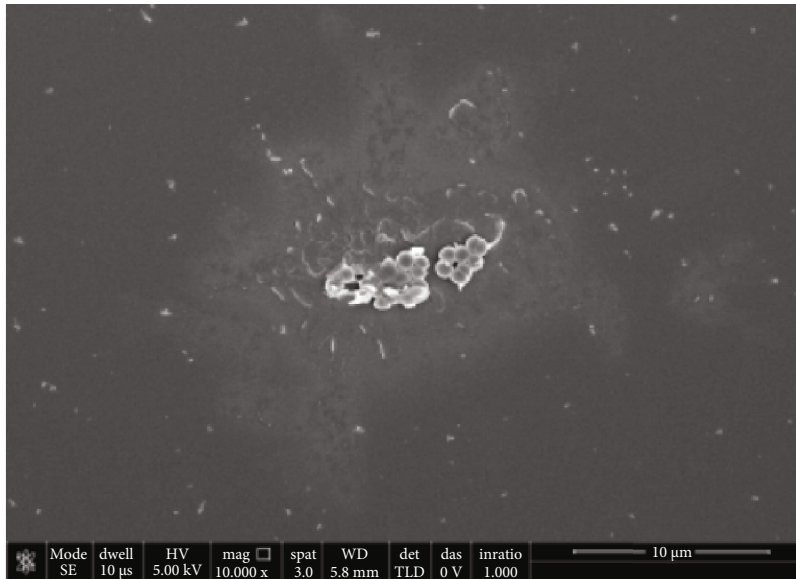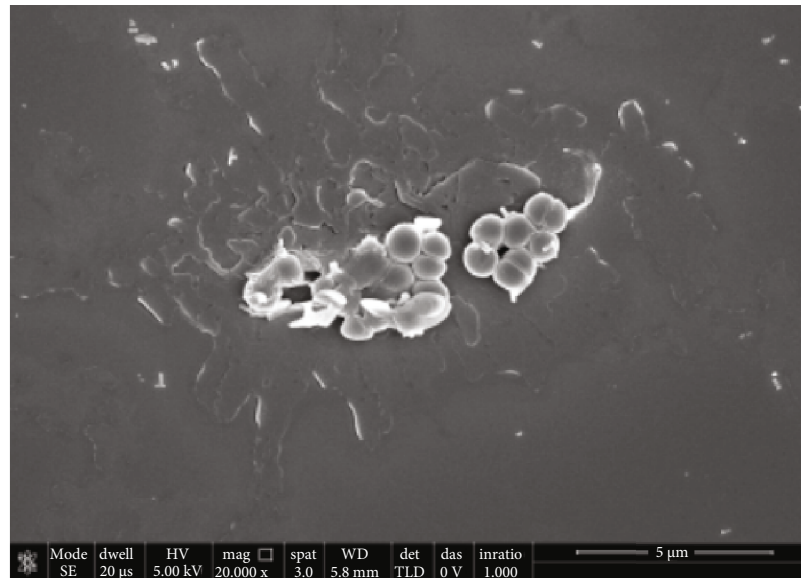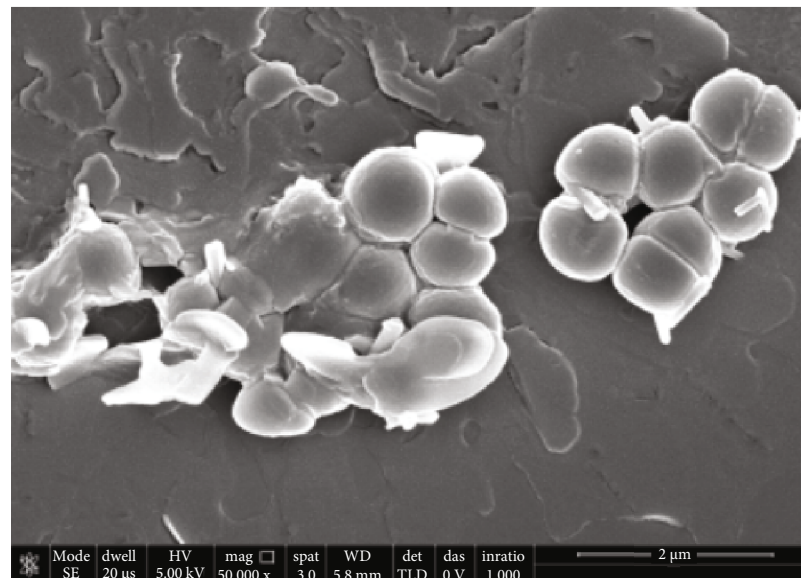| Mode | dwell | HV | mag ▫ | spat | WD | det | das | inratio | 5 μm |
| SE | 20 μs | 5.00 kV | 20.000 x | 3.0 | 5.6 mm | TLD | 0 V | 1.000 | |

(b)

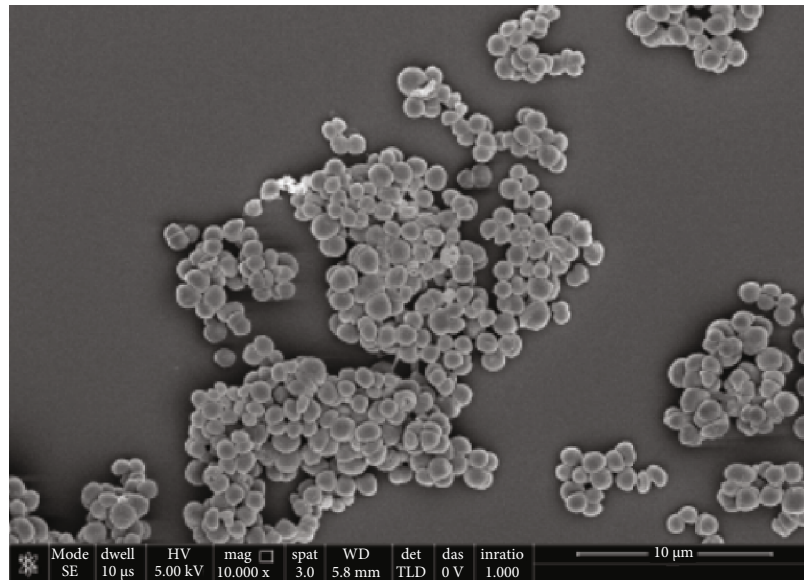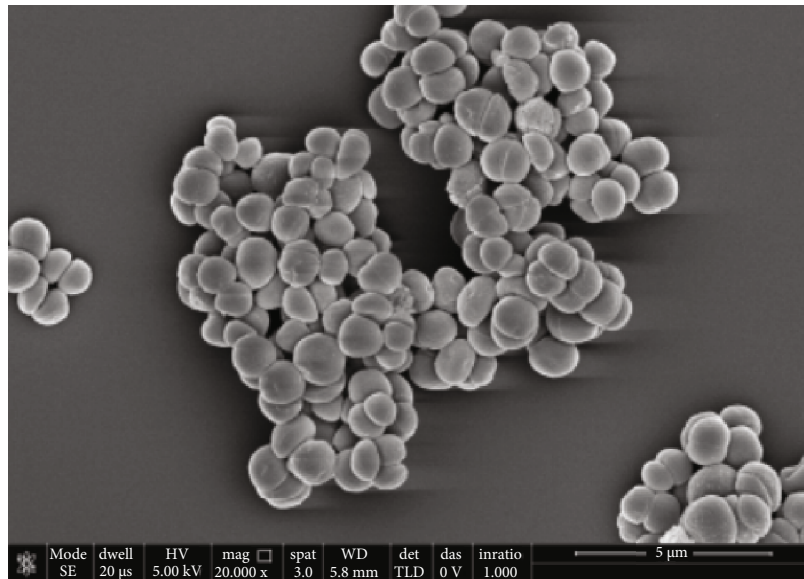FIGURE 3: Continued.

(c)

(d)

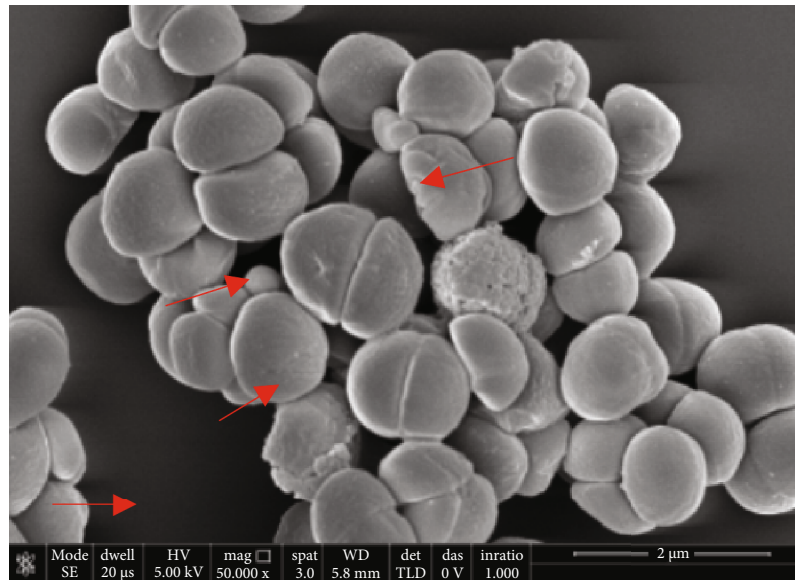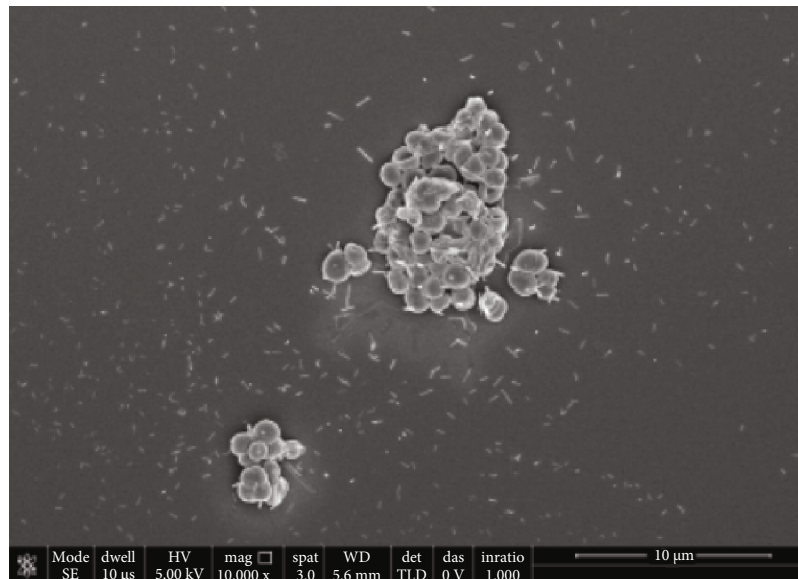FIGURE 3: Continued.

(e)

(f)
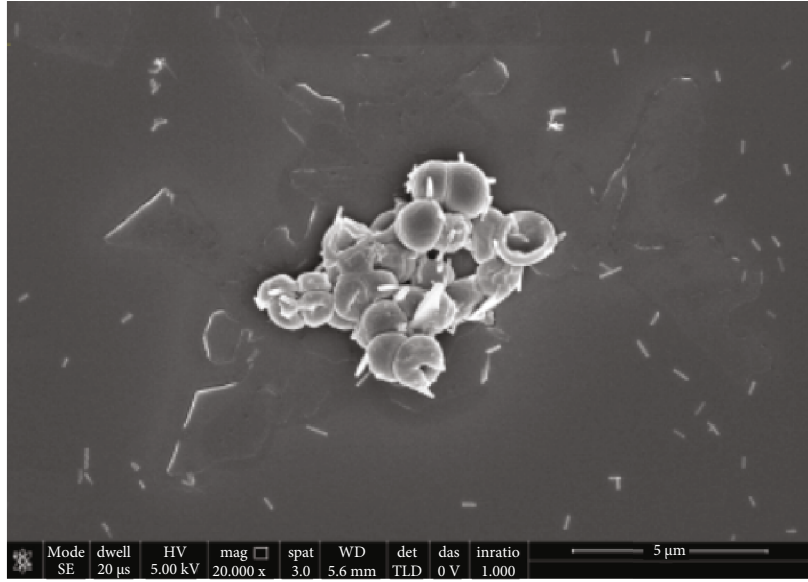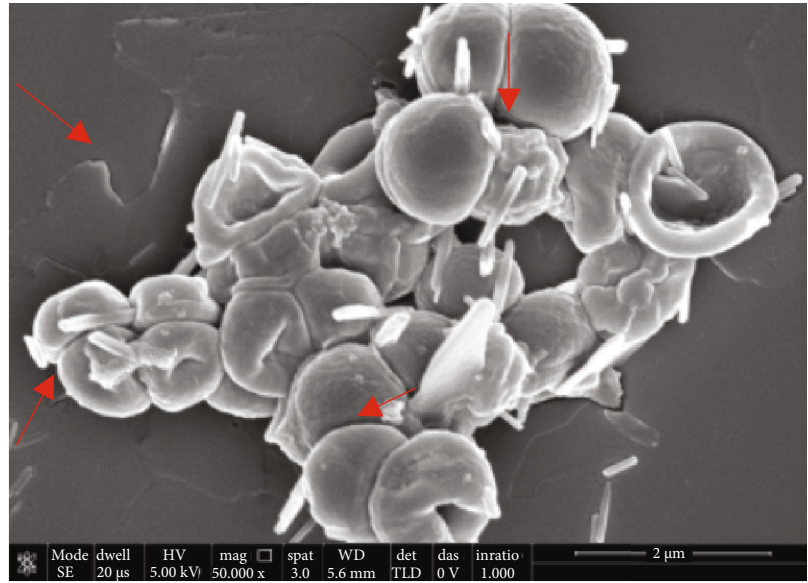
FIGURE 3: Continued.

(g)
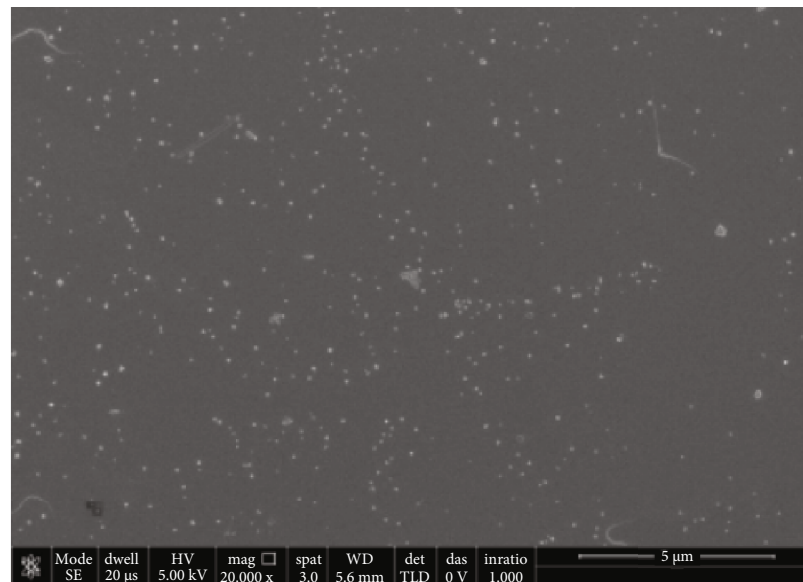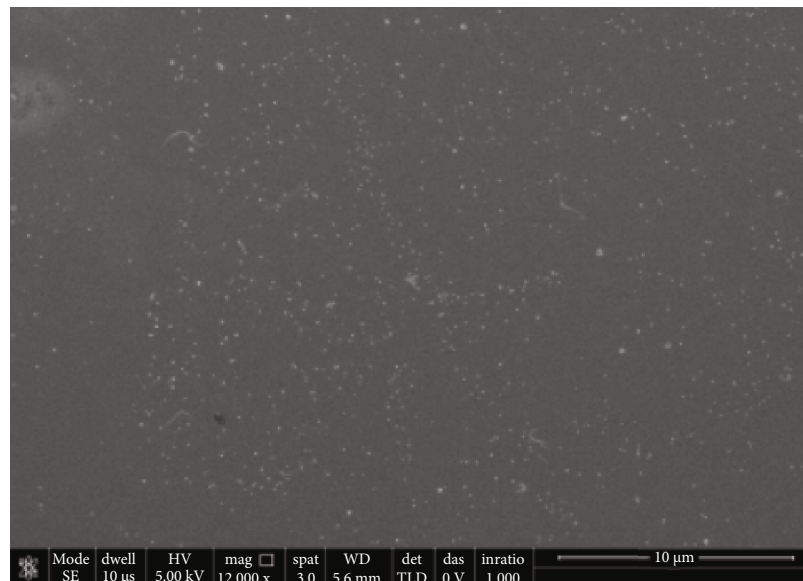

(h)

Figure 3: Continued.

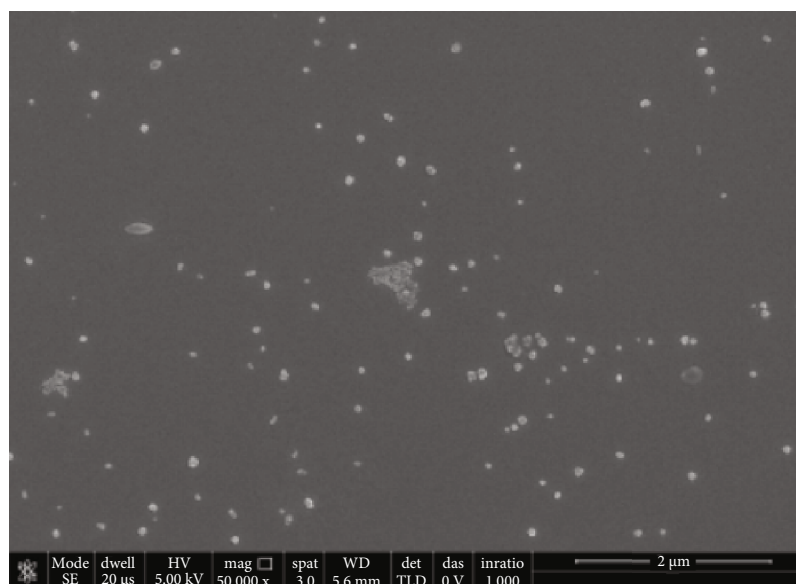(i)

(j)

FIGURE 3: Continued.

(k)

(l)

Figure 3: Continued.

(m)

(n)

FIGURE 3: Continued.

(o)

FIGURE 3: SEM analysis of (a–c) unexposed and (d–f) vancomycin (10.4 μg/mL) treated *S. epidermidis* ATCC 12228 planktonic cells. Bacterial treatment with doses of (g–i) 1/2× MIC, (j–l) 1× MIC, and (m–o) 2× MIC. For each sample, three different areas were acquired, and for each area, three different magnifications were applied (10.000×, 20.000×, and 50.000×).

concentrations tested, recording mortality rates of 70% and 85% at 50 and 100 μg/mL, respectively. However, at concentrations below 12.5 μg/mL, no relevant cytotoxicity was detected. To support the results, the hemolysis test confirmed 38% and 25% red blood cell lysis at the same concentrations after 2 h of exposure. For both assays, CTRL− represented by cells exposed to the solvent used to dissolve the drug (2% DMSO) did not undergo cellular alteration. In comparison, CTRL+ (represented by 100% DMSO in the MTT and 0.1% TritonX-100 in the hemolysis assay) induced a 100% mortality rate (Figures 1(a) and 1(b)). The CC_{50}, CC_{90}, HC_{50}, and HC_{90} values calculated according to the dose-response curve were 33.63, 121.55, 44.32, and 161.44 μg/mL, respectively.

3.2. In Vitro Antibacterial Property. A Kirby–Bauer disk diffusion test was performed to screen the antibacterial activity against several Gram-positive and Gram-negative bacteria. The inhibition area observed after exposure to 50 μg of teniposide was 21 ± 0.7, 22 ± 0.2, and 25 ± 0.1 mm against *E. faecalis*, *S. aureus*, and *S. epidermidis*, respectively. About Gram-negative bacteria, *K. pneumoniae* showed a slight susceptibility, registering an inhibition halo of 15 ± 0.2 mm, while *E. coli* and *S. enterica* ser. Typhimurium were not affected by growth. All strains were sensitive to CTRL+, with an inhibition zone in the range of 34–35 mm for linezolid (10 μg) and 17–16 mm for piperacillin (30 μg). Conversely, the solvent used to dissolve the compound (10 μL 100% DMSO) did not cause inhibition of bacterial growth (Figures 2(a), 2(b), 2(c), 2(d), 2(e), and 2(f)). The antibacterial efficacy of the drug was further investigated using the broth microdilution method. A dose-response curve was generated by exposing the selected bacteria to a 50–1.56 μg/mL drug concentration scale. Teniposide exhibited

a minimum concentration inhibiting 90% of growth (MIC_{90}) greater than 50 μg/mL for *E. coli*, S. *enterica* ser. Typhimurium, and *K. pneumoniae*; 12.5 μg/mL against *E. faecalis*; and 6.25 μg/mL against *S. aureus* and *S. epidermidis* (Figure 2(g)). Due to the higher teniposide sensitivity of *S.epidermidis* and its significant clinical impact, this strain underwent extensive investigation. First, the antimicrobial activity of teniposide was tested against 10 clinical isolates with broad resistance profiles, revealing a MIC_{90} value of 6.25 μg/mL, against all strains tested (data not shown).

After that, the kinetic action of teniposide was evaluated by performing a time-kill curve analysis against a reference strain and a clinical isolate (S_1). In both conditions, bacterial exponential growth over time was detected for bacteria not exposed to the compound. A feeble microbial growth impairment for the reference strain after treatment with 3.12 μg/mL (1/2× MIC) compared to the CTRL− occurred. Indeed, no growth alteration was reported in the clinical isolate at the same concentration. Conversely, 6 h of exposure to 6.25 μg/mL (1× MIC) and 12.5 μg/mL (2× MIC) induced a gradual reduction of the bacterial load, and after 20 h, no microbial growth was detected, indicating the bactericidal action of teniposide (Figures 2(h) and 2(i)).

To evaluate the bacterial morphological effect, a microscopic investigation was conducted on reference *S. epidermidis*, in response to teniposide treatment. The acquired SEM images indicated drug-induced surface differences. In detail, the unexposed bacteria showed the expected smooth and regular surfaces and spheroidal morphologies with an average diameter of ~1 μm. Treatment with vancomycin (CTRL+) induced complete cell lysis with widespread bacterial debris, and residual cells showed irregular shapes. The drug at a dose of 3.12 μg/mL (1/2× MIC) reduced the microbial load, and the planktonic cells showed morphological

PI   SYTO9   Merged
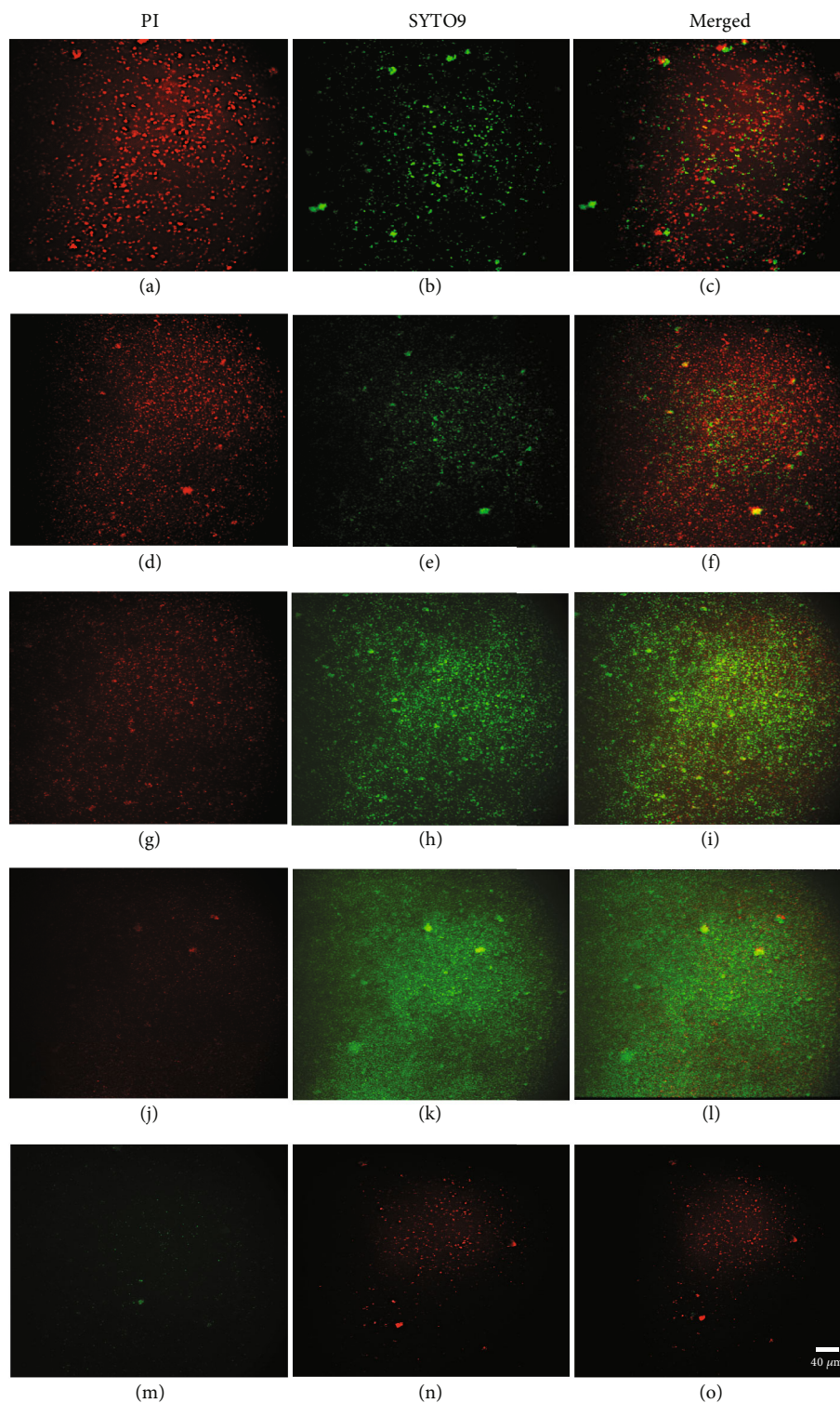
FIGURE 4: BacLight LIVE/DEAD staining after treatment of *S. epidermidis* ATCC 12228 with teniposide analyzed under a fluorescence microscope: (a–c) treatment with 12.5 μg/mL; (d–f) treatment with 6.25 μg/mL; (g–i) treatment with 3.12 μg/mL; (j–l) untreated bacteria; (m–o) bacteria treated with vancomycin.

alterations, with protuberances on the surface appearing rough for some cells, as indicated by the arrows. In support of the time-killing data, a few areas of high bacterial density and viable planktonic cells were highlighted after exposure to the 6.25 μg/mL (1× MIC) dose of the drug. Bacteria showed indentation, collapse, lysis, and nonintact cell morphology. Moreover, at double the MIC value (12.5 μg/mL), no intact cells were detected (Figures 3(a), 3(b), 3(c), 3(d), 3(e), 3(f), 3(g), 3(h), 3(i), 3(j), 3(k), 3(l), 3(m), 3(n), and 3(o)). To strengthen the evidence obtained, fluorescence

(a)

(b)

(c)

(d)

(e)

(f)

(g)

(h)

(i)

(j)
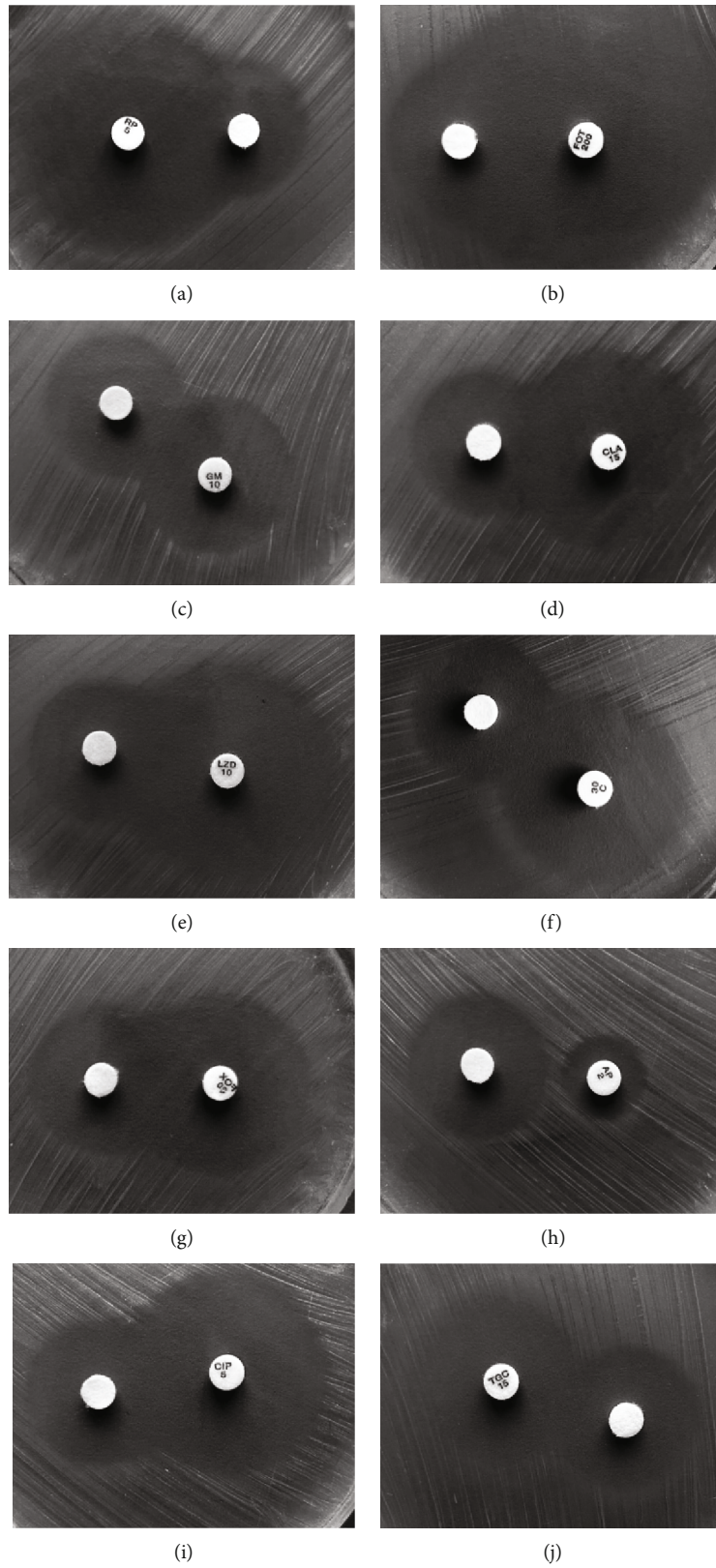
FIGURE 5: Continued.
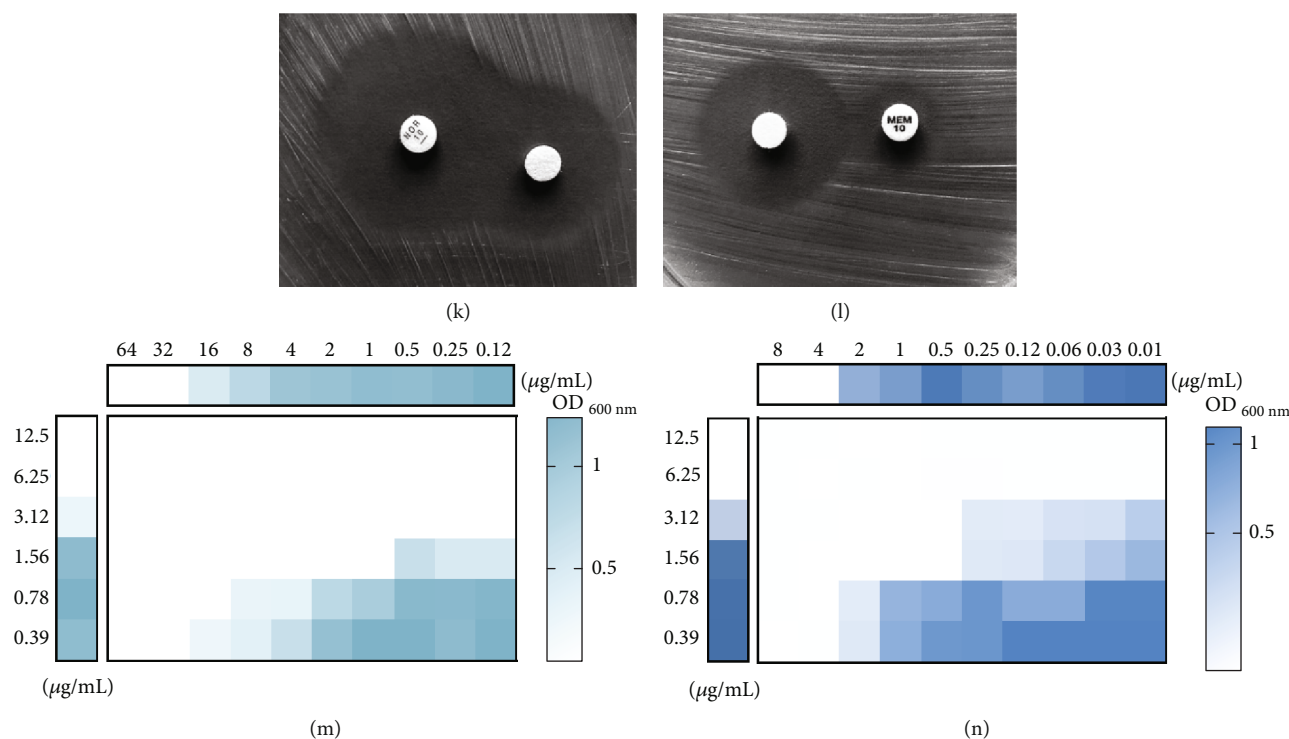
FIGURE 5: The combinatorial effect between teniposide (50 µg) and (a) rifampicin (5 µg), (b) fosfomycin (200 µg), (c) gentamicin (10 µg), (d) clarithromycin (15 µg), (e) linezolid (10 µg), (f) chloramphenicol (30 µg), (g) cefoxitin (30 µg), (h) ampicillin (2 µg), (i) ciprofloxacin (5 µg), (j) tigecycline (15 µg), (k) norfloxacin (10 µg), and (l) meropenem (10 µg). The drug–drug interactions were qualitatively evaluated after 20 h of incubation. (m) Fosfomycin and (n) gentamycin combinations were confirmed by checkerboard assays.

microscopy of LIVE/DEAD cells was conducted by staining with PI and SYTO-9 *S. epidermidis* reference strain. The cells permeable to PI and SYTO-9 are considered dead, while the membrane-intact cells permeable to SYTO-9 are considered viable. The cells were treated with a dose of 3.12 ($1/2\times$ MIC), 6.25 ($1\times$ MIC), and 12.5 µg/mL ($2\times$ MIC) of teniposide for 6 h. The results indicated a uniform viable bacterial density in the unexposed bacterial control, highlighted by the bright green fluorescent background, with some red traces representing physiological death. Planktonic bacteria treated with 12.5–6.25 µg/mL showed a reduction in cell density and cell damage, reflecting intense red staining. At the concentration of 3.12 µg/mL, a higher bacterial density and a reduction of dead cells were recorded by increasing the number of green-stained live cells. Few nonviable cells were observed after vancomycin treatment, accounting for CTRL+ (Figure 4(a), 4(b), 4(c), 4(d), 4(e), 4(f), 4(g), 4(h), 4(i), 4(j), 4(k), 4(l), 4(m), 4(n), and 4(o)).

3.3. Teniposide/Antibiotic Combination Assay.

To enhance the effectiveness of the conventional antibiotics, rifampicin (5 µg), fosfomycin (200 µg), gentamicin (10 µg), clarithromycin (15 µg), linezolid (10 µg), chloramphenicol (30 µg), cefoxitin (30 µg), ampicillin (2 µg), ciprofloxacin (5 µg), tigecycline (15 µg), norfloxacin (10 µg), and meropenem (10 µg) were combined with teniposide (50 µg) at an exact distance of 2 cm. Double-disk synergy tests conducted on *S. epidermidis* revealed that teniposide, when combined with rifampicin, fosfomycin, gentamicin, clarithromycin, linezolid, chloram-

phenicol, cefoxitin, ciprofloxacin, and norfloxacin, exhibited a potential additive/synergistic effect. Conversely, ampicillin, tigecycline, and meropenem did not cooperate additively/synergistically with the tested drug (Figures 5(a), 5(b), 5(c), 5(d), 5(e), 5(f), 5(g), 5(h), 5(i), 5(j), 5(k), and 5(l)). Based on the promising inhibition halos and readily available antibiotics, the checkerboard method was employed to confirm potential additivity/synergisms. Fosfomycin and teniposide demonstrated efficient synergism against *S. epidermidis*, proven by a FICI of 0.28. Similarly, gentamicin showed synergism with teniposide, corresponding to a FICI of 0.37 (Figures 5(m) and 5(n)). Otherwise, ciprofloxacin was associated with additivity, provided by a FICI of 0.52. Indeed, the teniposide–clarithromycin combination had indifferent behavior, with a FICI > 1 (data not shown).

3.4. Inhibition of Biofilm Matrix and Sessile Cell Metabolic Activity.

Biofilm formation represents one of the most concerning virulence factors associated with *S. epidermidis* catheter-related infections. Consequently, the impact of teniposide during the early (2 h) and late (24 h) phases of biofilm formation was investigated. Matrix biomass was quantified by the CV method in treated samples ranging from 50 to 0.39 µg/mL. The most relevant data were represented by the teniposide inhibitory capacity at $1/2\times$ MIC concentrations, which recorded 46–42–39% and 65–61–56.5% of matrix inhibition for *S. epidermidis* ATCC, S_1, and S_2 after 2 and 24 h, respectively. Considering the drug's bactericidal effect against planktonic cells, the ability of teniposide to
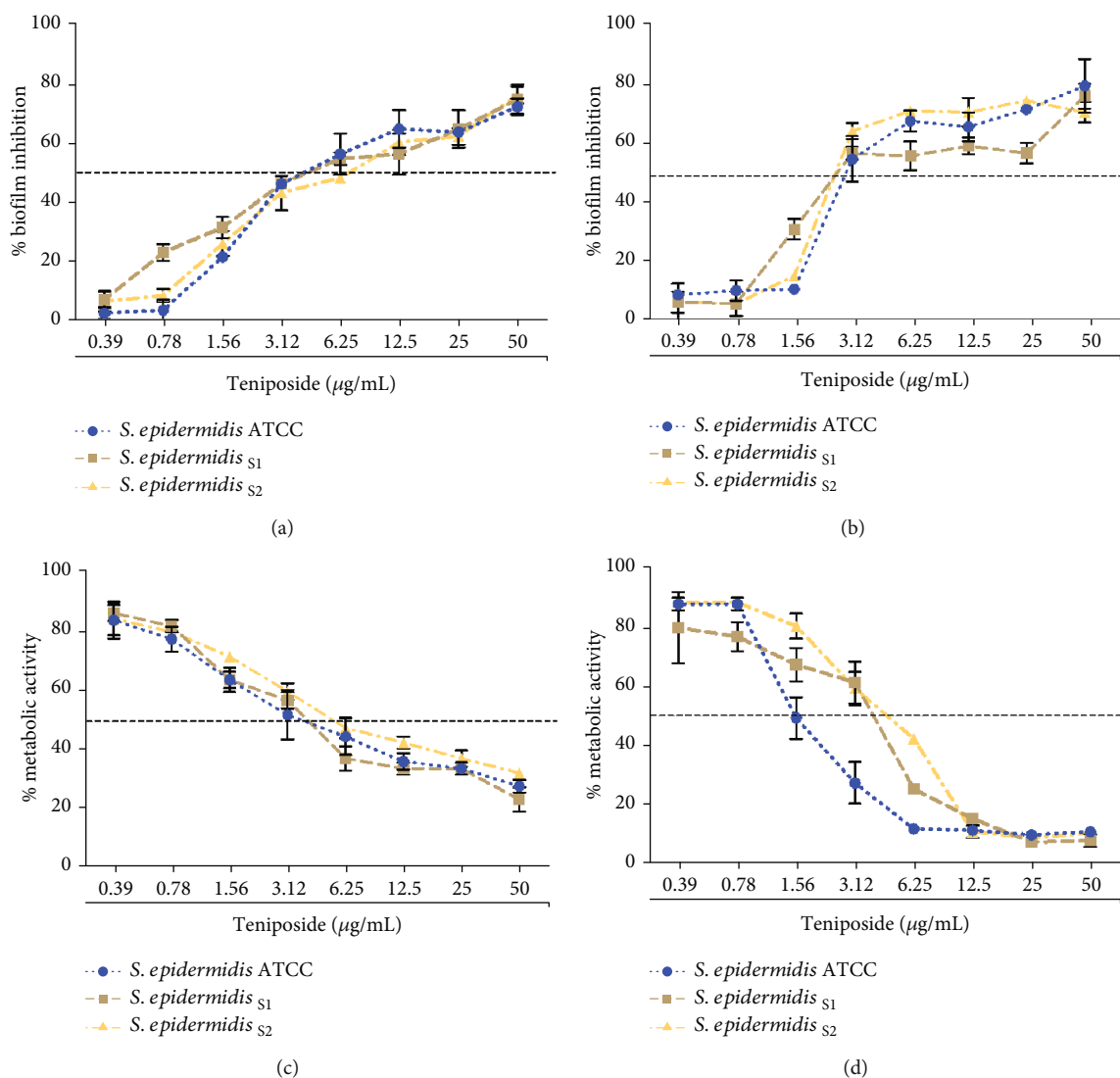
FIGURE 6: Impact of teniposide on the *S. epidermidis* ATCC, S_1, and S_2 biofilm matrix in the (a) early stages of attachment and (b) during the maturation stage. Impaired metabolic activity of sessile cells in inhibited biofilm (c) during the early stages of attachment and (d) in the maturation stage.

impair the metabolic activity of sessile cells was investigated by the MTT assay. According to the effects on the biomass of the biofilm, the same concentrations compromised the bacterial metabolism in a dose-dependent manner, showing metabolic activity of 51–63–60% and 23–24–25% after 2 and 24 h at the $1/2 \times$ MIC against sensible strains and clinical isolates, respectively (Figures 6(a), 6(b), 6(c), and 6(d)).

4. Discussion

S. epidermidis has garnered attention due to its emerging threat to healthcare [1]. Although previously considered a commensal bacterium, it has become necessary to categorize it as an opportunistic pathogen [33]. Its ability to adhere to medical devices and form biofilms has rendered it a challenging opponent of nosocomial infections [34]. Furthermore, *S. epidermidis* has demonstrated a remarkable propensity to develop antibiotic resistance through intrinsic

and acquired mechanisms [35, 36]. This highlights the critical need for innovative therapeutic strategies beyond conventional antibiotics to combat the growing threat posed by MDR *S. epidermidis*. Drug repurposing offers attractive advantages such as reduced development costs and shorter lead times. Drug repurposing has significant benefits, including reduced development costs and shorter timelines [37]. By taking advantage of the established safety profiles, pharmacokinetics, and known mechanisms of action of existing drugs, drug repurposing aims to evaluate their potential efficacy against alternative diseases. Our study operates within this framework, focusing on the antimicrobial properties of teniposide, which have not been extensively studied or thoroughly investigated [38–40]. Therefore, our study delved into the repurposing of FDA-approved teniposide as a potential antibacterial agent. It is a semisynthetic derivative of podophyllotoxin, a natural compound present in various plant sources [41]. It belongs to the class of topoisomerase

inhibitors and is mainly used as a chemotherapy drug to treat different types of cancer, especially leukemia [42]. Although its primary mode of action is associated with its antineoplastic properties, there is several evidences suggesting potential antimicrobial activity. An antibacterial screening study conducted by Chan et al. [43] demonstrated the inhibitory effects of teniposide against different strains, both Gram-negative and Gram-positive bacteria. However, no study to date has comprehensively elucidated the kinetics of action, effects on planktonic cells and biofilms, or potential synergistic interactions with other drugs. Therefore, we undertake a detailed exploration of the antibacterial properties of teniposide, starting with a broad-spectrum screening against both Gram-negative and Gram-positive bacteria. The drug, through diffusion in agar and the microdilution method, did not show a relevant ability to inhibit the growth of Gram-negative bacteria. However, its action was evident against Gram-positive bacteria, including *E. faecalis*, *S. aureus*, and *S. epidermidis*. The different activity observed in the two bacterial populations could be attributed to structural differences in their cell walls. Teniposide exhibited a MIC$_{90}$ value equal to $6.25\,\mu g/mL$, consistent with a previously mentioned study which reported a MIC value of $8\,\mu g/mL$ against *S. aureus* [43]. To confirm drug effectiveness, it was tested on 10 *S. epidermidis* clinical isolates, to demonstrate whether the drug acted independently of the resistance profile. The drug's activity over time and the induced morphological changes were examined through time-killing analysis and microscopic investigations. Teniposide induced a reduction in the bacterial load after 6 h of action, as evidenced by the high cellular permeability to PI, an indicator of degradation of cell membranes. After 20 h of pharmacological exposure, no viable cells were counted in the time-killing assay. Likewise, SEM analyses demonstrated the presence of residual bacterial populations with completely damaged morphology. These evidences irrefutably proved the bactericidal action of teniposide against *S. epidermidis*. Moreover, a possible strategy to prevent chronic infections is aimed at biofilm inhibition. Data relating to CV and MTT assay indicated that teniposide was able to inhibit biofilm formation in the early and maturation stages in a concentration-dependent manner. To date, no study has documented the ability of teniposide to counteract biofilm formation. Similarly, hydroxyapatite synthesized with etoposide showed a peculiar inhibition of biofilm formation, as documented by laser scanning confocal microscopy (CLSM) [44]. Although the cellular target of the drug is not currently known in prokaryotic cells, the mechanism of action of teniposide in eukaryotes involves its interaction with DNA and the Topoisomerase II enzyme [45]. As a result of the interaction between teniposide with Topoisomerase II, the enzyme becomes trapped in the DNA, forming the "cleavable complex" [46]. This complex consists of the enzyme covalently linked to DNA, with the broken DNA strands accumulating in cells. The latter triggers break–repair mechanisms, which the drug counteracts. DNA damage, replication, and transcription machinery stalling result in the activation of cell death pathways, mainly apoptosis. Topoisomerase II in bacteria is represented by the DNA gyrase, a possible target of teniposide in prokaryotes [47].

A study conducted on the drug etoposide (another semi-synthetic derivative of podophyllotoxin) showed cocrystalline structure activity against *S. aureus* DNA gyrase. DNA cleavage assay confirmed that etoposide stabilized both single-stranded (SSB) and double-stranded (DSB) breaks, demonstrating the inhibitory action of DNA gyrase. In addition, etoposide-stabilized SSB and DSB persisted over a wide range of concentrations ($800–12.5\,\mu M$) of etoposide with DNA gyrase [43]. In the second step of our study, the combinatorial effect of teniposide with different antibiotics was evaluated. Among the selected antibiotics, the combinations of teniposide/fosfomycin and teniposide/gentamicin were explored as promising combination therapies to enhance the efficacy of antimicrobial treatment (FICI < 0.37). This could be attributable to the different mechanisms of action: fosfomycin interferes with cell wall synthesis by inhibiting the initial stages of peptidoglycan biosynthesis, while gentamicin is an aminoglycoside antibiotic that impairs bacterial protein synthesis [48, 49]. The different targets of the drugs involved could explain the combined action of teniposide with the two antibiotics.

Overall, the reported evidence reinforces the idea that drug repurposing represents a promising strategy in the ongoing challenge against antimicrobial resistance. The worrying increase in antibiotic-resistant bacterial strains and the slow development of new antibiotics require advantageous approaches for the discovery of new molecules with antimicrobial properties [50]. Reusing drugs originally designed for different therapeutic purposes allows researchers to take advantage of shorter development times, well-established safety data, and well-understood pharmacokinetics [21]. However, the intricate mechanisms of microbial resistance and the complexity of host–drug interactions require thorough investigation to ensure the efficacy and safety of the repurposed molecules [51]. Further studies will be necessary to confirm the exact mechanism of action of teniposide, strengthening its potential use as an antibacterial agent.

Data Availability Statement

The authors have nothing to report.

Conflicts of Interest

The authors declare no conflicts of interest.

Author Contributions

Gianluigi Franci and Massimiliano Galdiero: conceptualization and writing—original draft preparation. Federica Dell'Annunziata and Veronica Folliero: methodology. Roberta Della Marca and Francesca Palma: formal analysis. Giuseppina Sanna: visualization. Anna De Filippis: visualization. Pasquale Pagliano and Aldo Manzin: project administration. Gianluigi Franci: writing—review and editing and supervision. Massimiliano Galdiero: writing—review and

editing and supervision. All authors have read and agreed to the published version of the manuscript.

Funding

Supporting Information

Additional supporting information can be found online in the Supporting Information section. Graphical abstract. Analysis of the antibacterial activity of teniposide against Gram-positive and negative bacteria by disk diffusion, broth dilution method, time-kill kinetics, LIVE/DEAD staining, and SEM. Evaluation of the inhibitory and degradative effects on the biofilm matrix and teniposide/antibiotic combination assay. Investigation of the cytotoxic action on the HaCaT cell line and human red blood cells. (*Supporting Information*)

References

[1] M. M. Severn and A. R. Horswill, "*Staphylococcus epidermidis* and its dual lifestyle in skin health and infection," *Nature Reviews Microbiology*, vol. 21, no. 2, pp. 97–111, 2023.

[2] M. Widerström, "Significance of Staphylococcus epidermidis in health care-associated infections, from contaminant to clinically relevant pathogen: this is a wake-up call!," *Journal of Clinical Microbiology*, vol. 54, no. 7, pp. 1679–1681, 2016.

[3] W. F. Oliveira, P. M. S. Silva, R. C. S. Silva et al., "*Staphylococcus aureus* and *Staphylococcus epidermidis* infections on implants," *The Journal of Hospital Infection*, vol. 98, no. 2, pp. 111–117, 2018.

[4] V. I. Martínez-Santos, D. A. Torres-Añorve, G. Echániz-Aviles, I. Parra-Rojas, A. Ramírez-Peralta, and N. Castro-Alarcón, "Characterization of *Staphylococcus epidermidis* clinical isolates from hospitalized patients with bloodstream infection obtained in two time periods," *PeerJ*, vol. 10, article e14030, 2022.

[5] K. Schilcher and A. R. Horswill, "Staphylococcal biofilm development: structure, regulation, and treatment strategies," *Microbiology and Molecular Biology Reviews*, vol. 84, no. 3, article e00026-19, 2020.

[6] M. E. Powers, P. A. Smith, T. C. Roberts et al., "Type I signal peptidase and protein secretion in *Staphylococcus epidermidis*," *Journal of Bacteriology*, vol. 193, no. 2, pp. 340–348, 2011.

[7] K. Perez and R. Patel, "Survival of *Staphylococcus epidermidis* in fibroblasts and osteoblasts," *Infection and Immunity*, vol. 86, no. 10, article e00237-18, 2018.

[8] I. Pastar, K. O'Neill, L. Padula et al., "*Staphylococcus epidermidis* boosts innate immune response by activation of gamma delta T cells and induction of perforin-2 in human skin," *Frontiers in Immunology*, vol. 11, p. 550946, 2020.

[9] L. M. Bebell and A. N. Muiru, "Antibiotic use and emerging resistance: how can resource-limited countries turn the tide?," *Global Heart*, vol. 9, no. 3, pp. 347–358, 2014.

[10] R. Chabi and H. Momtaz, "Virulence factors and antibiotic resistance properties of the *Staphylococcus epidermidis* strains isolated from hospital infections in Ahvaz, Iran," *Tropical Medicine and Health*, vol. 47, no. 1, p. 56, 2019.

[11] Z. Majeed, M. Qudir Javid, S. Nawazish et al., "Clinical prevalence, antibiogram profiling and gompertz growth kinetics of resistant *Staphylococcus epidermidis* treated with nanoparticles of rosin extracted from *Pinus roxburghii*," *Antibiotics*, vol. 11, no. 9, p. 1270, 2022.

[12] Y. Dutt, R. Dhiman, T. Singh et al., "The association between biofilm formation and antimicrobial resistance with possible ingenious bio-remedial approaches," *Antibiotics*, vol. 11, no. 7, p. 930, 2022.

[13] P. Shadvar, A. Mirzaie, and S. Yazdani, "Fabrication and optimization of amoxicillin-loaded niosomes: an appropriate strategy to increase antimicrobial and anti-biofilm effects against multidrug-resistant *Staphylococcus aureus* strains," *Drug Development and Industrial Pharmacy*, vol. 47, no. 10, pp. 1568–1577, 2021.

[14] V. Folliero, G. Franci, F. Dell'Annunziata et al., "Evaluation of antibiotic resistance and biofilm production among clinical strain isolated from medical devices," *International Journal of Microbiology*, vol. 2021, Article ID 9033278, 2021.

[15] M. B. Sannathimmappa, V. Nambiar, and R. Aravindakshan, "Antibiotics at the crossroads-do we have any therapeutic alternatives to control the emergence and spread of antimicrobial resistance?," *Journal of Education and Health Promotion*, vol. 10, no. 1, p. 438, 2021.

[16] D. M. Klug, F. I. M. Idiris, M. A. T. Blaskovich et al., "There is no market for new antibiotics: this allows an open approach to research and development," *Wellcome Open Research*, vol. 6, p. 146, 2021.

[17] Y. Cha, T. Erez, I. J. Reynolds et al., "Drug repurposing from the perspective of pharmaceutical companies," *British Journal of Pharmacology*, vol. 175, no. 2, pp. 168–180, 2018.

[18] A. Haddadian, F. F. Robattorki, H. Dibah et al., "Niosomes-loaded selenium nanoparticles as a new approach for enhanced antibacterial, anti-biofilm, and anticancer activities," *Scientific Reports*, vol. 12, no. 1, article 21938, 2022.

[19] T. I. Oprea, J. E. Bauman, C. G. Bologa et al., "Drug repurposing from an academic perspective," *Drug Discovery Today: Therapeutic Strategies*, vol. 8, no. 3–4, pp. 61–69, 2011.

[20] B. M. Sahoo, B. V. V. Ravi Kumar, J. Sruti, M. K. Mahapatra, B. K. Banik, and P. Borah, "Drug repurposing strategy (DRS): emerging approach to identify potential therapeutics for treatment of novel coronavirus infection," *Frontiers in Molecular Biosciences*, vol. 8, p. 628144, 2021.

[21] Z. Y. Low, I. A. Farouk, and S. K. Lal, "Drug repositioning: new approaches and future prospects for life-debilitating diseases and the COVID-19 pandemic outbreak," *Viruses*, vol. 12, no. 9, p. 1058, 2020.

[22] F. Lüke, D. C. Harrer, P. Pantziarka et al., "Drug repurposing by tumor tissue editing," *Frontiers in Oncology*, vol. 12, p. 900985, 2022.

[23] F. Dell'Annunziata, S. Cometa, R. Della Marca et al., "In vitro antibacterial and anti-inflammatory activity of arctostaphylos uva-ursi leaf extract against *Cutibacterium acnes*," *Pharmaceutics*, vol. 14, no. 9, p. 1952, 2022.

[24] V. Folliero, F. Dell'Annunziata, E. Roscetto et al., "Rhein: a novel antibacterial compound against *Streptococcus mutans* infection," *Microbiological Research*, vol. 261, p. 127062, 2022.

[25] V. Folliero, F. Dell'Annunziata, E. Roscetto et al.et al., "Niclosamide as a repurposing drug against *Corynebacterium striatum* multidrug-resistant infections," *Antibiotics*, vol. 11, no. 5, p. 651, 2022.

[26] V. Folliero, F. Dell'Annunziata, B. Santella et al., "Repurposing selamectin as an antimicrobial drug against hospital-acquired *Staphylococcus aureus* infections," *Microorganisms*, vol. 11, no. 9, p. 2242, 2023.

[27] R. S. Gupta, A. Bromke, D. W. Bryant, R. Gupta, B. Singh, and D. R. McCalla, "Etoposide (VP16) and teniposide (VM26): novel anticancer drugs, strongly mutagenic in mammalian but not prokaryotic test systems," *Mutagenesis*, vol. 2, no. 3, pp. 179–186, 1987.

[28] J. L. Grem, D. F. Hoth, B. Leyland-Jones, S. A. King, R. S. Ungerleider, and R. E. Wittes, "Teniposide in the treatment of leukemia: a case study of conflicting priorities in the development of drugs for fatal diseases," *Journal of Clinical Oncology: Official Journal of the American Society of Clinical Oncology*, vol. 6, no. 2, pp. 351–379, 1988.

[29] K. Hevener, T. A. Verstak, K. E. Lutat, D. L. Riggsbee, and J. W. Mooney, "Recent developments in topoisomerase-targeted cancer chemotherapy," *Acta Pharmaceutica Sinica B*, vol. 8, no. 6, pp. 844–861, 2018.

[30] H. Li, T. Li, L. Zhang et al., "Antimicrobial compounds from an FDA-approved drug library with activity against *Streptococcus suis*," *Journal of Applied Microbiology*, vol. 132, no. 3, pp. 1877–1886, 2022.

[31] F. Dell'Annunziata, V. Folliero, F. Palma et al., "Anthraquinone rhein exhibits antibacterial activity against *Staphylococcus aureus*," *Applied Sciences*, vol. 12, no. 17, p. 8691, 2022.

[32] F. Palma, F. Dell'Annunziata, V. Folliero et al., "Cupferron impairs the growth and virulence of *Escherichia coli* clinical isolates," *Journal of Applied Microbiology*, vol. 134, no. 10, article lxad222, 2023.

[33] M. Otto, "*Staphylococcus epidermidis*–the 'accidental' pathogen," *Nature Reviews Microbiology*, vol. 7, no. 8, pp. 555–567, 2009.

[34] L. Montanaro, P. Speziale, D. Campoccia et al., "Scenery of *Staphylococcus* implant infections in orthopedics," *Future Microbiology*, vol. 6, no. 11, pp. 1329–1349, 2011.

[35] M. G. Eladli, N. S. Alharbi, J. M. Khaled, S. Kadaikunnan, A. S. Alobaidi, and S. A. Alyahya, "Antibiotic-resistant *Staphylococcus epidermidis* isolated from patients and healthy students comparing with antibiotic-resistant bacteria isolated from pasteurized milk," *Saudi Journal of Biological Sciences*, vol. 26, no. 6, pp. 1285–1290, 2019.

[36] W. C. Reygaert, "An overview of the antimicrobial resistance mechanisms of bacteria," *AIMS Microbiology*, vol. 4, no. 3, pp. 482–501, 2018.

[37] D. Paul, G. Sanap, S. Shenoy, D. Kalyane, K. Kalia, and R. K. Tekade, "Artificial intelligence in drug discovery and development," *Drug Discovery Today*, vol. 26, no. 1, pp. 80–93, 2021.

[38] E. Asadipour, M. Asgari, P. Mousavi, T. Piri-Gharaghie, G. Ghajari, and A. Mirzaie, "Nano-biotechnology and challenges of drug delivery system in cancer treatment pathway: review article," *Chemistry & Biodiversity*, vol. 20, no. 6, article e202201072, 2023.

[39] E. Kort and S. Jovinge, "Drug repurposing: claiming the full benefit from drug development," *Current Cardiology Reports*, vol. 23, no. 6, p. 62, 2021.

[40] F. Rezaie Amale, S. Ferdowsian, S. Hajrasouliha et al., "Gold nanoparticles loaded into niosomes: a novel approach for enhanced antitumor activity against human ovarian cancer," *Advanced Powder Technology*, vol. 32, no. 12, pp. 4711–4722, 2021.

[41] Z. Shah, U. F. Gohar, I. Jamshed et al., "Podophyllotoxin: history, recent advances and future prospects," *Biomolecules*, vol. 11, no. 4, p. 603, 2021.

[42] J. L. Delgado, C.-M. Hsieh, N.-L. Chan, and H. Hiasa, "Topoisomerases as anticancer targets," *The Biochemical Journal*, vol. 475, no. 2, pp. 373–398, 2018.

[43] P. F. Chan, V. Srikannathasan, J. Huang et al., "Structural basis of DNA gyrase inhibition by antibacterial QPT-1, anticancer drug etoposide and moxifloxacin," *Nature Communications*, vol. 6, no. 1, article 10048, 2015.

[44] V. Ganesan, G. Meiyazhagan, M. Devaraj et al., "Repurposing the antibacterial activity of etoposide–a chemotherapeutic drug in combination with eggshell-derived hydroxyapatite," *ACS Biomaterials Science & Engineering*, vol. 8, no. 2, pp. 682–693, 2022.

[45] A. M. Wilstermann, R. P. Bender, M. Godfrey et al., "Topoisomerase II-drug interaction domains: identification of substituents on etoposide that interact with the enzyme," *Biochemistry*, vol. 46, no. 28, pp. 8217–8225, 2007.

[46] J. L. Nitiss, "Targeting DNA topoisomerase II in cancer chemotherapy," *Nature Reviews. Cancer*, vol. 9, no. 5, pp. 338–350, 2009.

[47] M. Pietrusiński and P. Staczek, "Bacterial type II topoisomerases as targets for antibacterial drugs," *Postepy Biochemii*, vol. 52, no. 3, pp. 271–282, 2006.

[48] K. M. Krause, A. W. Serio, T. R. Kane, and L. E. Connolly, "Aminoglycosides: an overview," *Cold Spring Harbor Perspectives in Medicine*, vol. 6, no. 6, article a027029, 2016.

[49] A. S. Michalopoulos, I. G. Livaditis, and V. Gougoutas, "The revival of fosfomycin," *International Journal of Infectious Diseases*, vol. 15, no. 11, pp. e732–e739, 2011.

[50] M. Terreni, M. Taccani, and M. Pregnolato, "New antibiotics for multidrug-resistant bacterial strains: latest research developments and future perspectives," *Molecules*, vol. 26, no. 9, p. 2671, 2021.

[51] Y. Liu, Z. Tong, J. Shi, R. Li, M. Upton, and Z. Wang, "Drug repurposing for next-generation combination therapies against multidrug-resistant bacteria," *Theranostics*, vol. 11, no. 10, pp. 4910–4928, 2021.